Estimating Suppression of Eddy Mixing by Mean Flows

Citation: Klocker, Andreas, Raffaele Ferrari, and Joseph H. LaCasce. "Estimating Suppression of Eddy Mixing by Mean Flows." Journal of Physical Oceanography 42.9 (2012): 1566–1576. ©2013 American Meteorological Society

As Published: http://dx.doi.org/10.1175/jpo-d-11-0205.1

Publisher: American Meteorological Society

Persistent URL: http://hdl.handle.net/1721.1/78643

Version: Final published version: final published article, as it appeared in a journal, conference proceedings, or other formally published context

Estimating Suppression of Eddy Mixing by Mean Flows

ANDREAS KLOCKER* AND RAFFAELE FERRARI

Massachusetts Institute of Technology, Cambridge, Massachusetts

JOSEPH H. LACASCE

Department of Geosciences, University of Oslo, Oslo, Norway

(Manuscript received 2 November 2011, in final form 27 March 2012)

ABSTRACT

Particle- and tracer-based estimates of lateral diffusivities are used to estimate the suppression of eddy mixing across strong currents. Particles and tracers are advected using a velocity field derived from sea surface height measurements from the South Pacific, in a region west of Drake Passage. This velocity field has been used in a companion paper to show that both particle- and tracer-based estimates of eddy diffusivities are equivalent, despite recent claims to the contrary. These estimates of eddy diffusivities are here analyzed to show 1) that the degree of suppression of mixing across the strong Antarctic Circumpolar Current is correctly predicted by mixing length theory modified to include eddy propagation along the mean flow and 2) that the suppression can be inferred from particle trajectories by studying the structure of the autocorrelation function of the particle velocities beyond the first zero crossing. These results are then used to discuss how to compute lateral and vertical variations in eddy diffusivities using floats and drifters in the real ocean.

1. Introduction

Eddy transport across mean currents is a central element in many phenomena, such as in the poleward movement of warm waters in the Southern Ocean and the lateral spreading of nutrient-rich waters in upwelling zones. Understanding this transport, and parameterizing it in coarse-resolution climate models, is of great interest at present (e.g., Toole and McDougall 2001).

Often the eddies responsible for transport derive from the instability of a mean current, such as the Antarctic Circumpolar Current (ACC) in the Southern Ocean or the California Current over the western slope of North America. This suggests that eddy transport is greatest near the mean current itself, as eddy mixing scales with eddy kinetic energy (EKE; Prandtl 1925; Holloway 1986). However, there is a growing body of evidence suggesting that the mean flow also suppresses mixing (e.g., Bower et al. 1985; Nakamura and Ma 1997; Haynes and Shuckburgh 2000a,b; Allen and Nakamura 2001; Marshall et al. 2006; Abernathey et al. 2010; Ferrari and Nikurashin 2010). Thus assessing cross-jet transport involves finding the balance between the enhancement of mixing by instability and the suppression imposed by the mean.

The present study seeks to improve this understanding by considering mixing in a theoretical model and by measuring mixing with a realistic velocity field. The work builds on the study of Ferrari and Nikurashin (2010), extending the theoretical work to particles and by addressing mixing at depth in addition to that at the surface. It also follows a companion paper, Klocker et al. (2012, hereafter KFLM), in which tracer- and particle-based diffusivities were compared.

The present focus is on the Southern Ocean. We show that mixing is suppressed across the core of the ACC: that is, from the surface down to 1500 m. Mixing is greater to the north of the ACC and below it. As suggested by the theoretical model, the suppression of the diffusivity is associated with the drift of eddies with respect to the mean flow. This is manifested in a negative lobe in the particle autocorrelation function. Accurate diffusivity estimates thus require that this lobe be taken into account.

* Current affiliation: Research School of Earth Sciences, The Australian National University, Canberra, ACT, Australia.

Corresponding author address: Andreas Klocker, Research School of Earth Sciences, The Australian National University, Canberra ACT 0200, Australia.
E-mail: andreas.klocker@anu.edu.au

DOI: 10.1175/JPO-D-11-0205.1

The paper is organized as follows: The theoretical model is derived in section 2. The velocity field, derived from fields in the Southern Ocean, is discussed in section 3. Tracer-derived diffusivities are examined in section 4a and compared directly to the theoretical model. Particle-based estimates are examined in section 4b, and recommendations are made for observational studies. The work concludes with section 5.

2. Theory

To illustrate the suppression of mixing across a jet, we follow Ferrari and Nikurashin (2010) and represent eddy mixing as a stochastically forced wave equation. Ferrari and Nikurashin (2010) found that such a model, when used to advect a passive tracer, successfully reproduces the meridional variation of the eddy diffusivity deduced using Nakamura's (1996) technique applied to surface geostrophic velocities. Here we examine the particle-based (Lagrangian) diffusivities derived using a similar stochastic flow.

We represent the ocean as an equivalent-barotropic fluid, governed by the quasigeostrophic potential vorticity (QGPV) equation,

$$\partial_t q + U\partial_x q + (\partial_y Q)\partial_x \psi + J(\psi, q) = 0, \tag{1}$$

where J is the Jacobian operator, ψ is the geostrophic streamfunction representing the wave motions, and

$$q = \nabla^2\psi - F\psi \tag{2}$$

is the associated potential vorticity (Pedlosky 1987). In the latter, $\nabla^2\psi$ and $F\psi$ represent the relative and stretching vorticities, respectively; $F = 1/\lambda^2$ is the inverse square of the deformation radius. The waves are imbedded in a mean zonal flow U and a large-scale PV gradient $\partial_y Q = \beta + FU$, where β is the planetary gradient of PV and the FU is the contribution by the mean flow shear (in an equivalent-barotropic model U is the difference between the flow in the active layer and the quiescent abyss, so it is a proxy for the vertical shear). Curvature terms associated with the bending of the mean flow are neglected, consistent with the assumption that the mean flow varies on scales much larger than the waves.

We express the streamfunction in terms of its Fourier transform,

$$\psi(x, y, t) = \frac{1}{2}\sum_k \sum_l a(t)e^{ikx+ily} + \text{c.c.}, \tag{3}$$

where c.c. denotes the complex conjugate. The evolution of the amplitude a is obtained by substituting (3) into (1),

$$\frac{d}{dt}a + ikc_w a = \mathcal{N}, \tag{4}$$

where $\mathcal{N}$ is a nonlinear function, proportional to the transform of the advective term, and where

$$c_w = U + c, \quad c = -\frac{\partial_y Q}{\kappa^2 + F}, \tag{5}$$

with $\kappa^2 = k^2 + l^2$ being the square of the total wavenumber. Here, c is the free phase speed of the baroclinic Rossby wave and c_w is the Doppler shifted Rossby wave speed that would be measured with a Hovmöller diagram of the streamfunction. Thus, (4) governs the evolution of Rossby waves forced by eddy interactions, represented by $\mathcal{N}$ (deriving, e.g., from baroclinic instability).

Analytical solutions to (4) can be obtained if one replaces $\mathcal{N}$ with a fluctuation–dissipation stochastic forcing term, because this effectively linearizes the PV equation. There is an extensive literature on such models (e.g., Farrell and Ioannou 1993; Flierl and McGillicuddy 2002; DelSole 2004) wherein these representations are described. The particular form we will use is

$$\mathcal{N} = -\frac{2\mathcal{U}\sqrt{\gamma}}{\kappa}r(t) - \gamma a. \tag{6}$$

The fluctuations are generated by a white noise random process $r(t)$, with zero mean and an autocorrelation $\langle r(t)r^*(t')\rangle = \delta(t - t')$ (where $\langle\cdot\rangle$ denotes the expected value and the star is the complex conjugate). The amplitude of the forcing is determined by the constant $\mathcal{U}$. The dissipation is represented as a linear damping term acting on the potential vorticity (a choice of simplicity rather than realism). Thus, the evolution equation for the streamfunction amplitude a is

$$\frac{d}{dt}a + ikc_w a + \gamma a = -\frac{2\mathcal{U}\sqrt{\gamma}}{\kappa}r(t). \tag{7}$$

The solution to (7) is

$$a(t) = \frac{2\mathcal{U}\sqrt{\gamma}}{\kappa}\int_0^\infty r(t - \tau)e^{-\gamma\tau - ikc_w\tau}\, d\tau. \tag{8}$$

The form of the RHS is chosen to omit the initial condition, which is irrelevant in what follows. Given this, the kinetic energy of the eddy field is

$$\text{EKE} \equiv \frac{1}{2}\left(\overline{|\partial_x\psi|^2} + \overline{|\partial_y\psi|^2}\right) = \frac{1}{2}\mathcal{U}^2, \tag{9}$$

where the bars indicate a spatial average over the lateral domain. The result explains our choice of amplitude in (6).

With the eddy streamfunction, we can derive relations for the motion of particles advected by the field. Because

our focus is on mixing across the zonal mean current, we will concentrate on meridional displacements. Following Taylor (1921), we can define a diffusivity in the meridional direction,

$$K_{1y}(x,y,t) = \frac{1}{2}\frac{d}{dt}\langle\eta^2\rangle = \int_0^t R(t',t)\,dt', \qquad (10)$$

where the integrand in the last term,

$$R(t,t') \equiv \langle v_L(t;x,y,t)v_L(t';x,y,t)\rangle, \qquad (11)$$

is the autocorrelation of the meridional Lagrangian velocity. Here, $v_L(t';\,x,\,y,\,t)$ is the velocity at time t' of a particle that passes through (x, y) at time t. Because the eddy field produced by the stochastic model is stationary, the autocorrelation only depends on the difference between t' and t,

$$R(t,t') = R(t - t'), \qquad (12)$$

and we can accordingly replace the $v_L(t;\,x,\,y,\,t)$ with $v_L(0;\,x,\,y,\,0)$ in (11) without loss of generality. Furthermore, as the eddy field is homogeneous, we can replace the ensemble average with an integral over space and the autocorrelation becomes independent of position.

For small-amplitude eddies, particles simply drift zonally at the speed U and one can easily compute the Lagrangian velocity from the Eulerian one,

$$v_L(t';x,y,0) = v(x - Ut',y,t'). \qquad (13)$$

Although this relationship is valid only if one ignores, at leading order, the particle motions induced by the eddies, the resulting autocorrelation appears to hold for finite-amplitude eddies as well, as noted hereafter. Armed with this relationship, the transformed Lagrangian meridional velocity for the stochastically driven flow is

$$\begin{aligned} v_L(t';x,y,0) &= \left.\frac{\partial\psi}{\partial x}\right|_{(x-Ut',y,t')} \\ &= \frac{1}{2}ika(t')e^{ik(x-Ut')+ily} + \text{c.c.} \end{aligned} \qquad (14)$$

with the amplitude a given in (8). We calculate the autocorrelation thus as

$$R_{vv}(t') = \langle v(x - Ut',y,t')\,v(x,y,0)\rangle. \qquad (15)$$

Substituting in the full expression for v, we obtain

$$R_{vv} = \frac{k^2\mathcal{U}^2\gamma}{\kappa^2}\left[\int_0^\infty d\tau'\int_0^\infty d\tau\,\langle r(t' - \tau')r^*(t - \tau)\rangle e^{-\gamma(\tau+\tau')+ik(c_w-U)(\tau-\tau')} + \text{c.c.}\right], \qquad (16)$$

where c.c. is the complex conjugate of the preceding double integral. Using the fact that

$$\langle r(t' - \tau')r^*(t - \tau)\rangle = \delta(t' - \tau' - t + \tau), \qquad (17)$$

(16) reduces to

$$R_{vv}(t') = \frac{k^2\mathcal{U}^2}{\kappa^2}e^{-\gamma t'}\cos[k(c_w - U)t']. \qquad (18)$$

The autocorrelation decays exponentially in time, with a time scale proportional to γ^{-1}, the inverse of the linear damping coefficient. At the same time R oscillates, with a frequency of $k(c_w - U) = kc$. If the decay and oscillation time scales are comparable, the autocorrelation exhibits an exponential decay at small lags and a pronounced negative lobe at larger lags (as seen below). If the decay time scale is slower than the period of the oscillations, then the autocorrelation oscillates with many positive and negative lobes.

The meridional diffusivity is the integral of the autocorrelation. It is straightforward to show that this has a long-time asymptote of

$$\lim_{t\to\infty} K_{1y} = \frac{k^2}{\kappa^2}\frac{\gamma\mathcal{U}^2}{\gamma^2 + k^2(c_w-U)^2}. \qquad (19)$$

Thus, the character of the autocorrelation and the size of the diffusivity depend on $c_w - U = c$. If $c = 0$, the diffusivity is proportional to the EKE times the eddy decorrelation time scale γ^{-1}. This is what one would conclude from the mixing length theory (Prandtl 1925). With a nonzero c, the autocorrelation oscillates with lag and the diffusivity is suppressed.

The phase speed c is proportional to the mean PV gradient, $\partial_y Q = \beta + FU$. Thus, c is likely large in jets where the surface PV gradient is large, whereas it is smaller and possibly zero on the flanks of jets where the surface PV gradient is weak. Critical layers where $c = 0$ can only arise at the lateral flanks of jets in the equivalent-barotropic mode, but they arise also in the vertical where $c_w - U(z) = 0$ in the real ocean if the mean flow decays with depth. The Rossby wave speed of the equivalent-barotropic model must be interpreted as the surface phase speed $c = c_w - U(0)$. Ferrari and Nikurashin (2010) show that (19) holds also for vertically varying flows, if one substitutes the depth-dependent eddy

kinetic energy $\mathcal{U}(z)^2$ in the numerator and the depth-dependent vertical velocity $U(z)$ in the denominator, whereas $c_w = U(0) + c$ remains the surface Doppler shifted wave speed. Hence, more generally the suppression of K_{1y} vanishes also in the vertical at critical layers where $c_w = U(z)$. Such levels are the steering levels of baroclinic instability and must exist if the jet is to be baroclinically unstable (e.g., Pedlosky 1987). Thus, one expects large $c_w - U$ in the upper core of jets and strong suppression of mixing. On the lateral and vertical flanks, $c_w - U$ is instead weaker and mixing is not suppressed. In regions where the mean flow is weak, the mean PV gradient is just β and c is the slow (westward) phase speed of the baroclinic Rossby wave and there is little suppression of mixing.

If we define K^0_{1y} to be the eddy diffusivity for eddies with $c = 0$, then (19) can be written as

$$K_{1y} = \frac{K^0_{1y}}{1 + k^2(c_w - U)^2/\gamma^2}. \tag{20}$$

This shows that the reduction in K is proportional to the ratio of the decorrelation time scale γ^{-1} over the advection time scale $1/k(c_w - U) = 1/kc$.

Interestingly, one arrives at the same result if one considers a passive tracer (Ferrari and Nikurashin 2010). Assuming a mean zonal flow and a mean meridional gradient for the tracer, Γ, this is

$$\frac{\partial C}{\partial t} + U\frac{\partial C}{\partial x} + J(\psi, C) + \Gamma v = 0, \tag{21}$$

where ψ is the eddy streamfunction obtained above. The solution is obtained by calculating the correlation between C and the meridional velocity and then dividing the result by the mean gradient Γ. The result is the same as the particle-based estimate in (19) and is equivalent to that obtained by Ferrari and Nikurashin (2010) [their Eq. (12)].[1] The only difference is that $c_w - U$ in their model is the intrinsic phase speed of Eady waves propagating on the mean temperature gradient, because they use a surface quasigeostrophic model instead of an equivalent-barotropic model. The present diffusivity is recovered if the Eady wave is replaced with a baroclinic Rossby wave. The tracer-based solution is obtained by assuming the tracer has the same structure as the eddy field, so that the Jacobian of ψ and C vanishes. Ferrari and Nikurashin (2010) do not linearize the problem to derive the expression for the diffusivity in (20). This suggests that one may be able to obtain our result without linearizing the Lagrangian velocity in terms of the mean Eulerian flow.

Green (1970) also derives a similar expression for the eddy diffusivity for potential vorticity in horizontally homogeneous, baroclinically unstable flow based on the fastest growing linear normal mode. We review the argument and discuss the connection to the present model in the appendix.

Thus, the tracer- and particle-derived diffusivities agree. Such agreement was found in the numerical experiments of KFLM. It is also implicit in the results of Shuckburgh and Haynes (2003), who compared probability density functions (PDFs) for tracers and particles using a kinematic model.

One can also compare the present approach with previous studies using stochastic models for particle advection. In particular, the ''first order stochastic model with spin'' examined by Veneziani et al. (2004) yields an autocorrelation function that is the product of a decaying exponential and an oscillatory function. In this model, the stochastic forcing is applied directly to the particle velocity, and the oscillatory behavior comes from a rotational term coupling the velocities in the x and y directions. Veneziani et al. (2004) determined the rotational frequency by studying the motion of looping float trajectories in the Gulf Stream region.

The two approaches are complimentary. However, the philosophy is slightly different. In the stochastic model, the random forcing is applied directly to the particles and the ''spin'' is imposed to reproduce looping float trajectories. The approach is thus kinematic. In the present model, the stochastic forcing represents the action of eddies in the potential vorticity equation; the particles are simply advected by the flow. This clarifies the physical basis for the looping motion of the particles and shows that the suppression of eddy diffusivities in the ocean is the result of eddy propagation.

3. The velocity field

To study the modulation of eddy mixing across a mean current, we construct a velocity field representative of the ACC using the geostrophic streamfunction as measured from altimeters. This is the same velocity field used in a companion paper (KFLM); we will provide a summary here, but the reader is referred to KFLM for a more detailed description.

The sea level anomaly maps come from the combined processing of Ocean Topography Experiment (TOPEX), *European Remote Sensing Satellite-1* (*ERS-1*), and *ERS-2* altimetry data, and the mean streamlines are computed using the zonal mean of the sum of the mean geoid and

[1] Equation (19) corrects an inconsequential factor of 2 that did not appear in Eq. (12) of Ferrari and Nikurashin (2010).

a 3-yr time-mean sea surface height from altimetry. The sea level data has a temporal resolution of 10 days and a spatial resolution of ¼° longitude × ¼° latitude. We then use the geostrophic relation to derive geostrophic velocities at the ocean surface and interpolate the velocities onto a 1/10° grid to advect tracers and floats. We construct two different velocity fields: an eddy velocity field, in which we only use sea surface height anomalies to calculate geostrophic velocities, and a full velocity field, in which we add the zonal average of the zonal mean flow (ignoring the weak meridional mean flow).

We focus on a region upstream of Drake Passage between 103° and 78°W and between 30° and 66°S, the same region studied by the ongoing Diapycnal and Isopycnal Mixing Experiment in the Southern Ocean (DIMES). To calculate horizontal velocities below the surface, we assume an equivalent-barotropic structure of the ACC as suggested by Killworth and Hughes (2002); that is, we scale the surface geostrophic velocity by a structure function $\mu(z)$. This structure function is calculated from the output of the Southern Ocean State Estimate (SOSE; Mazloff et al. 2010), an eddy-permitting general circulation model of the Southern Ocean constrained to observations in a least squares sense. Using the surface geostrophic velocity field and the structure function, we construct a three-dimensional map of geostrophic velocities.

This equivalent-barotropic map of geostrophic velocities has several advantages over using the full three-dimensional velocity field from numerical models such as SOSE: 1) it provides a simple kinematic framework to test our theory (e.g., we can easily modify the mean flow without affecting the phase speed of the eddies) and 2) we can easily increase the resolution of the numerical code used to advect floats and tracers, so as to minimize spurious numerical diffusion. Even though this velocity field is highly idealized, it captures the key kinematic properties of the full velocity field and it generates eddy diffusivities very similar to those estimated by Abernathey et al. (2010), who computed diffusivities advecting tracers with the SOSE three-dimensional velocity field.

The advection of tracers and floats in this geostrophic velocity field is purely horizontal (i.e., vertical velocities are neglected). A correction is imposed to eliminate the weak lateral convergences associated with upwelling and downwelling: the correction consists in adding a divergent term to the altimetric velocity so that the resulting velocity field is divergenceless and satisfies no-normal-flow conditions at the north–south boundaries and periodic conditions at the east–west boundaries (for more details, see Marshall et al. 2006). This adjustment is very small and it is appreciable only close to the domain boundaries at the north and south.

4. Suppression of eddy diffusivity across the Antarctic Circumpolar Current

The equivalent-barotropic velocity field based on altimetric measurements and SOSE is now used to advect numerical floats and tracers. The tracer distributions are used to calculate effective diffusivity as defined by Nakamura (1996),

$$K_e = \frac{\kappa}{L_0^2(y)} \frac{\frac{\partial}{\partial A}\int |\nabla c|^2 \, dA}{\left(\frac{\partial C}{\partial A}\right)^2}, \tag{22}$$

where C is a tracer contour encircling the area A, κ is the numerical diffusivity used to advect the tracer, and $L_0(y)$ is the zonal extent of the domain at the latitude y (technically the equivalent latitude as defined in Shuckburgh and Haynes 2003). The float trajectories are used to calculate the meridional single-particle diffusivity K_{1y} as defined in Taylor (1921) and Davis (1991),

$$K_{1y} = \frac{1}{2}\frac{d}{dt}\langle (y(t) - y_0)^2 \rangle, \tag{23}$$

where $y(t)$ is the latitude of a particle released at y_0 at $t = 0$ and $\langle \cdot \rangle$ is the average over all particles released at y_0.

We only consider cross-ACC diffusivities, because Nakamura's approach is not well suited for computing along-current diffusivities. In the Pacific sector considered, the ACC is primarily along latitude lines and hence the analysis is in terms of meridional diffusivities.

KFLM show that K_e and K_{1y} are indistinguishable if one uses a sufficient number of floats. Here we consider both estimates to illustrate how mixing suppression across strong currents affects tracer and float statistics.

a. Tracer-based estimates

The results from the stochastic model suggest that the latitudinal variations in eddy diffusivity are best interpreted as a competition between the enhancement of mixing by eddy stirring and suppression by mean flow advection. We test this hypothesis by running two sets of calculations. In the first set, the tracer is advected by the full velocity field. In the second set, the tracer is advected by the eddy velocity only; that is, by the full velocity minus the zonal mean ACC flow.

Estimates of K_e from the tracer distributions obtained from the two calculations are shown in Fig. 1. In the absence of advection by the mean flow, K_e peaks in the core of the ACC, where the EKE is largest. This is consistent with mixing length scalings which posit that the eddy diffusivity is proportional to a mixing length scale times the square root of the EKE (Holloway 1986;

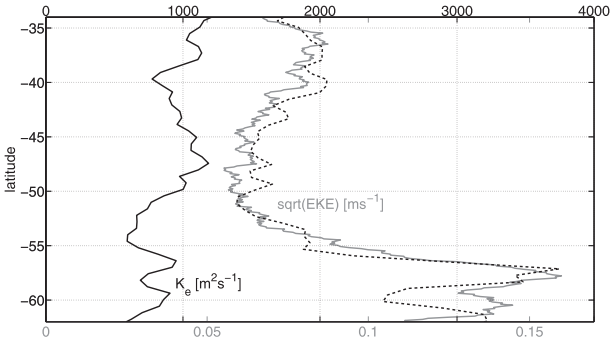

FIG. 1. Effective diffusivity K_e estimated from a tracer advected with the altimetric velocity field for an ACC sector upstream of Drake Passage between 103° and 78°W and between 30° and 66°S (black solid line). The black dashed line is the effective diffusivity for a tracer advected only with the velocity anomalies (i.e., subtracting the zonal mean velocity for the ACC sector considered). The gray line shows the square root of EKE and illustrates that the effective diffusivity tracks the square root of EKE only if one ignores advection by the mean zonal ACC flow.

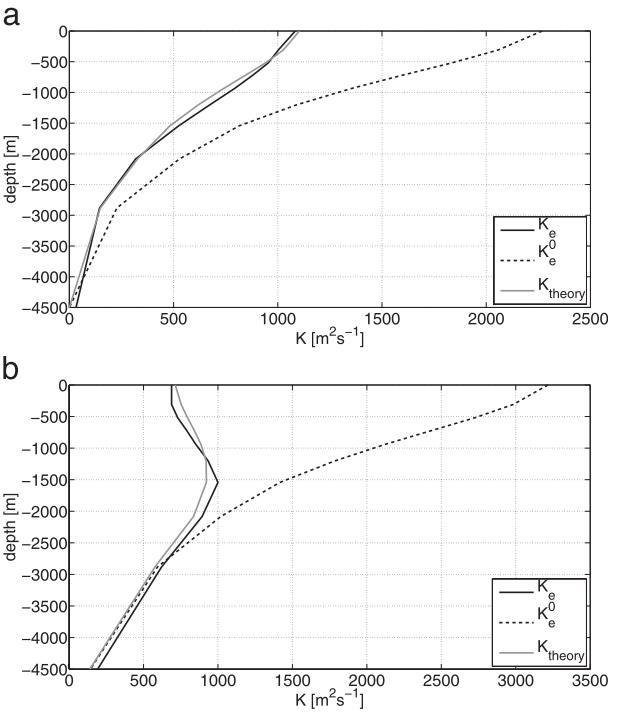

FIG. 2. (a) Zonal mean vertical profiles of effective diffusivity K_e averaged over the 44°–46°S latitude stripe north of the ACC and between 103° and 78°W (solid back line). The dashed black line shows K_e^0 from simulations where the mean flow is set equal to the eddy speed, so that eddy propagation does not suppress cross-current mixing. The gray line is obtained dividing K_0 by the suppression factor predicted by (20). (b) As in (a), but for the 58°–60°S latitude stripe in the core of the ACC.

Keffer and Holloway 1988). The addition of a mean flow, however, greatly reduces K_e, consistent with the theory outlined in section 2. The suppression is most pronounced in the ACC where the mean flow is largest.

Ferrari and Nikurashin (2010) show that the degree of suppression of the diffusivity by the ACC is captured qualitatively and quantitatively by the scaling in (20) based on the stochastic model. Here, we test the stochastic model throughout the full water column (Ferrari and Nikurashin 2010 considered only the ocean surface). We calculate K_e at 10 levels between the surface and 4500 m using the surface geostrophic velocity field scaled according to the equivalent-barotropic structure function $\mu(z)$.

Two sample vertical profiles of K_e are shown as black solid lines in Fig. 2 (the other lines in the figure are discussed later), one for a region north of the ACC between 44° and 46°S and the other for a region in the core of the ACC between 58° and 60°S (for full latitude–depth maps of eddy diffusivities, see KFLM). In the core of the ACC, the eddy diffusivity is suppressed by the mean flow at the surface and has a subsurface maximum around 1500 m, where the mean flow is weak. To the north, where the mean is weaker, the diffusivity is largest at the surface where the EKE is largest.

To test whether these profiles are consistent with the model in (20), four parameters must be estimated at each latitude and depth:[2] U, c_w, K_e^0, and γ/k. Figure 3 shows the surface mean flow U (solid line), which is defined to be the zonally averaged velocity (there is no significant meridional velocity in the Pacific sector we study) and the zonal phase speed of sea surface height eddy anomalies c_w (dashed line) estimated as we are about to explain. The mean velocity at any other depth is obtained by multiplying the surface velocity by $\mu(z)$. The other three parameters are harder to estimate, because the oceanic eddy field is multichromatic with a wide range of eddy sizes, propagation speeds, and decorrelation times (Wunsch 2010). Departing from previous literature that relies on somewhat arbitrary metrics to estimate mean representative values of these parameters (e.g., Tulloch et al. 2009), we use an approach better suited for analysis of eddy diffusivities. At each depth, we run a series of simulations where the tracer is advected by the velocity field $\mathbf{u} = \mathbf{u}_{\text{eddy}} + U_{\text{const}}\mathbf{i}$, where $\mathbf{u}_{\text{eddy}}$ is the depth-dependent eddy velocity, U_{const} is a constant zonal mean velocity independent of latitude and depth, and $\mathbf{i}$ is the zonal unit vector. The set of simulations use a mean velocity between -0.1 and 0.1 m s^{-1}. Sample curves of K_e as a function of U_{const} are

[2] K_e^0 is the effective diffusivity for eddies propagating at the same speed as the mean flow and it is equivalent to K_{1y}^0 in (19). We verified that K_e^0 and K_{1y}^0 are equivalent within error bars, but in the experiments below we use K_e^0 because it is easier to compute.

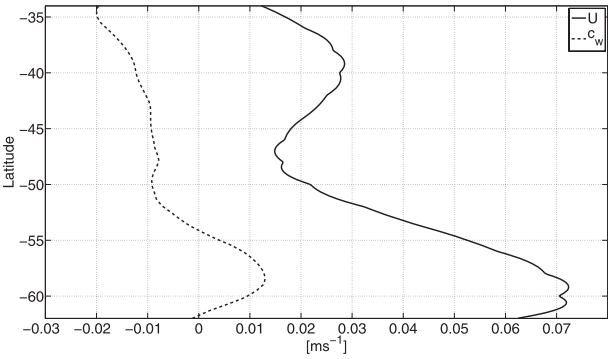

FIG. 3. Zonal mean surface velocity U (solid line) and zonal phase speed of sea surface height anomalies c_w (dashed line) for the same ACC sector used in Fig. 1.

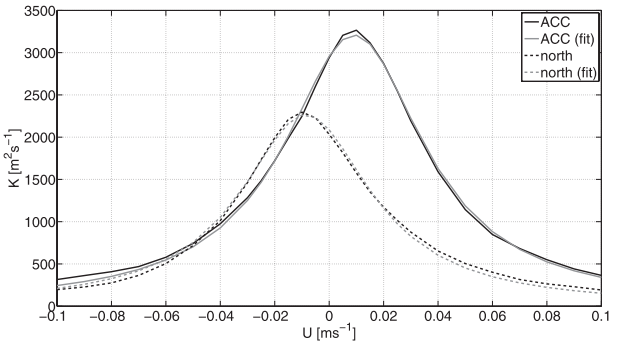

FIG. 4. Effective diffusivity K_e for a sector between 103° and 78°W north of the ACC between 44° and 46°S (dashed lines) and in the core of the ACC between 58° and 60°S (solid lines). The effective diffusivity is computed advecting a tracer with the sum of the altimetric velocity field anomalies and a constant zonal mean flow U_{const}; a separate simulation is run for each value of U_{const}. The black lines are the results of the calculation, the gray lines are least squares fit of (20) to the two curves of K_e vs U_{const}. These least squares fits are used to determine the parameters in the theoretical expression for the diffusivity.

shown in Fig. 4 for the two regions at the ocean surface, in the core of the ACC and north of it. The dependence of K_e on U_{const} has the Lorentzian shape predicted by (20) and can be used to estimate all the parameters we need. The curve maximum corresponds to K_e^0 and it is achieved when $U_{\text{const}} = c_w$. The curve width can be used to estimate γ/k.

These three parameters, c_w, K_e^0, and γ/k, are now estimated for each latitude and depth by least squares fitting the Lorentzian K_e curves to (20). Figure 4 shows that substituting the best-fit parameters in (20) reproduces the Lorentzian K_e curves remarkably well.

Our best-fit estimates suggest that eddies propagate eastward at $c_w \simeq +1$ cm s^{-1} in the core of the ACC and westward at $c_w \simeq -1$ cm s^{-1} north of it. These values are somewhat smaller than reported by Marshall et al. (2006), who estimated the speed of the most energetic eddies from altimetric data in the Southern Ocean. The discrepancy suggests the eddies that dominate eddy mixing are not the most energetic ones. The eddies that dominate mixing are instead somewhat slower and larger than the most energetic ones. This is consistent with mixing length arguments applied to multichromatic fields: the overall mixing is not dominated by eddies with the largest EKE but by eddies with the largest product of mixing length times EKE (e.g., Rose 1977; Holloway and Kristmannsson 1986). As long as the mixing length increases with the scale of the eddies, the product is expected to peak at scales somewhat larger than the scale at which EKE peaks.

Ferrari and Nikurashin (2010) argue that the decorrelation time scale of eddies γ^{-1} is proportional to the eddy turnover time, $(k^2\text{EKE})^{-1/2}$. This scaling is expected to hold for turbulent eddy fields with energy peaking at wavenumber k (Ottino 1998). We find that our estimates of γ/k do scale with the square root of EKE, but only in the upper 2000 m. The scaling breaks down at depth, where γ/k becomes depth independent, despite the decrease in EKE. Eddy stirring below 2000 m, where EKE is small, is probably best characterized as a superposition of time-dependent quasi-linear waves rather than a turbulent eddy field. This limit is generally referred to as chaotic mixing and the decorrelation time scale is not set by the eddy turnover time (Ottino 1989). In summary, our best fit of γ/k as a function of depth is

$$\frac{\gamma}{k} = \alpha_0 + \alpha_1\sqrt{\text{EKE}(z)}, \tag{24}$$

where α_0 and α_1 vary with latitude (primarily because the eddy scale changes with latitude).

Figure 2 summarizes the results. The vertical profile of the effective diffusivity K_e is plotted for the two regions, one in the core of the ACC and the other north of it. The figure also shows K_e^0 : that is, the effective diffusivity in the absence of any suppression due to eddy propagation. In both regions K_e^0 is substantially larger than K_e in the upper 2000 m, whereas $K_e \simeq K_e^0$ below. The suppression is largest in the ACC region especially at the surface where the eddy propagation speed, $c_w \simeq +1$ cm s^{-1}, is much smaller than the mean flow speed, $U \simeq +7$ cm s^{-1}. Figure 2 further shows that dividing K_e^0 by $[1 + (k^2/\gamma^2)(U - c_w^2)]$ recovers K_e very well; that is, (20) together with best estimates of U, c_w, and γ/k captures well the suppression of eddy mixing due to eddy propagation with respect to the mean flow.

Note that our goal is not to derive a closure scheme for eddy diffusivities. Rather we seek a theoretical model to interpret the vertical and horizontal variations in the

diffusivities. We will show that the same model can be used to interpret Lagrangian estimates of eddy mixing and provides clues on why previous studies failed to capture suppression of mixing by mean flows when relying on the dispersion of floats.

b. Float-based estimates

The stochastic model shows that the negative lobes in the Lagrangian velocity autocorrelations are directly linked to suppression of mixing by eddy propagation. The negative lobe is most pronounced when the period of oscillation of the cosine term in (18), $2\pi/|U - c_w|$, is shorter than the exponential decay time scale: that is, the eddy decorrelation time scale γ^{-1} or

$$|U - c_w| \geq 2\pi\frac{\gamma}{k}. \tag{25}$$

Otherwise, the velocity correlation decays exponentially to zero with hardly any oscillation. Using the best estimates of γ/k and $(U - c_w)$, we can now verify whether the negative lobes in R_{vv} are most pronounced when (25) is satisfied. This would further support our claim that the suppression of eddy mixing can be inferred from Lagrangian trajectories provided that the number of trajectories is large enough to accurately compute the negative lobes in R_{vv}.

In section 3, we estimated that in the ACC sector considered (bin centered at 59°S) $\gamma/k \simeq 0.03$ m s^{-1} and $|U - c_w| \simeq 0.06$ m s^{-1}, whereas to the north (bin centered at 45°S) $\gamma/k \simeq 0.03$ m s^{-1} and $|U - c_w| \simeq 0.03$ m s^{-1}. Hence, $|U - c_w| > \gamma/k$ in the ACC, leading to a large negative lobe in R_{vv}. North of the ACC, $|U - c_w| \simeq \gamma/k$ and the negative lobe is less pronounced. The width of the negative lobes of the Lagrangian autocorrelation function scales as $\pi/k|U - c_w|$ as per (18). In the ACC latitude band, eddies have scales of approximately 100 km, and hence $k \approx 2\pi/100$ km^{-1}. This gives a negative lobe of 20 days, a value consistent with the width of the negative lobe of R_{vv} in Fig. 5a (solid line). For comparison, Fig. 5a (dashed line) shows R_{vv} computed from trajectories advected by the eddy velocity field only (i.e., no mean); the negative lobe is much less pronounced because in these simulations $|c_w| < \gamma/k$. The single-particle diffusivities corresponding to these Lagrangian velocity autocorrelations are shown in Fig. 5b.

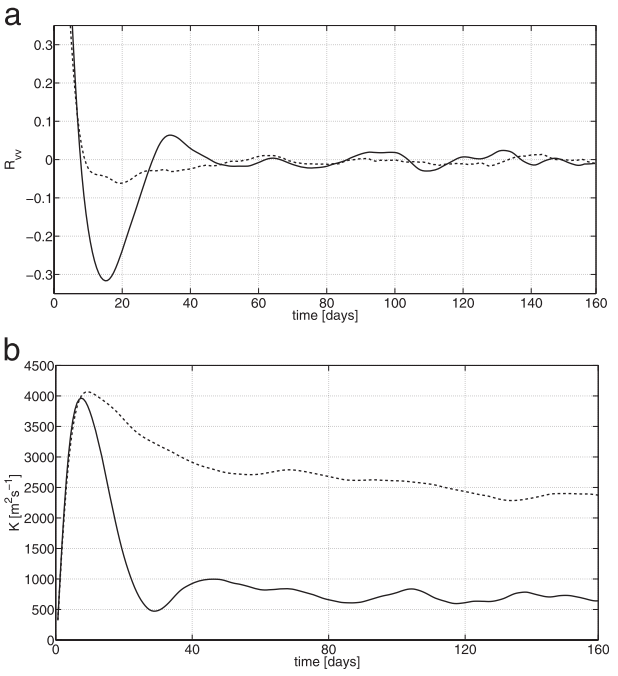

FIG. 5. (a) The Lagrangian velocity autocorrelation and (b) the corresponding single particle diffusivities for an ACC sector between 103° and 78°W and between 44° and 46°S. The solid lines are computed from numerical floats advected with the full altimetric velocity field, whereas the dashed lines are computed from numerical floats advected with the eddy altimetric velocity field: that is, the full velocity minus its zonal mean over the sector.

5. Summary and discussion

We computed lateral eddy diffusivities using tracers and floats advected by a proxy velocity field to study the suppression of eddy mixing by eddy propagation along mean flows. We focused on a region in the Southern Ocean, upstream of Drake Passage, which is the region of a large field experiment, the Diapycnal and Isopycnal Mixing Experiment in the Southern Ocean (DIMES). The main goal of DIMES is to quantify both isopycnal and diapycnal diffusivities in the Southern Ocean. In a companion paper (KFLM), we have shown that eddy diffusivities calculated using tracer and particle-based approaches are equivalent. In this manuscript, we used these lateral and vertical profiles of eddy diffusivities 1) to study what suppresses eddy mixing across mean flows and 2) to identify what statistics from float observations are robust markers of mixing suppression. The latter point is especially relevant to DIMES, because a primary aim is to estimate eddy diffusivities and their variations from the release of neutrally buoyant floats.

We addressed point 1 using mixing length arguments together with the eddy diffusivities calculated from the proxy velocity field. Traditional mixing length arguments assume that the eddy diffusivity is proportional to the eddy kinetic energy times a mixing length (e.g., Prandtl 1925). In the oceanographic literature, it is often assumed that the mixing length scales with the eddy size (e.g., Holloway 1986), but Ferrari and Nikurashin (2010) found that

propagating eddies reduce the mixing length and thereby play a crucial role in determining the variations in eddy diffusivity across the ocean. We extended the model here to study Lagrangian estimates of diffusivity. We find, in particular, that the latter is identical to the tracer-based estimate, confirming the numerical results of KFLM.

Abernathey et al. (2010) and KFLM found that eddy diffusivities are smaller than 1000 $m^2\ s^{-1}$ in the core of the ACC from the surface down to 1500 m but are larger than 1000 $m^2\ s^{-1}$ at depth and on the lateral flanks. Ferrari and Nikurashin (2010) interpret this pattern as evidence that mixing is suppressed in the core of the ACC, where eddies propagate slower than the mean current: eddies propagate eastward at a few centimeters per second, whereas the mean current flows at $O(10)$ cm s^{-1}. On the flanks of the ACC and at depth, the mean current speed is weaker and comparable to the eddy speed. These are the critical layers where there is no suppression of mixing.

To test the suppression of mixing by eddy propagation along mean flows, we ran a series of experiments with an eddy-only velocity field (i.e., the geostrophic velocity field calculated from sea surface height anomalies) and then added a constant zonal mean velocity independent of depth and latitude. By changing the mean velocity, we changed the relative speed between the eddies and the mean flow. We found that the eddy diffusivities computed for different mean flows closely followed the scaling law derived in Ferrari and Nikurashin (2010). That is, the spatial variations in eddy diffusivities estimated by KFLM can be explained by mixing length arguments, if the drift of the eddies with respect to the mean flow is taken into account.

Next, we focused on how to estimate the suppression of mixing using observations. Presently the only feasible approach to sample eddy diffusivities in the global ocean is by releasing drifters and floats (tracer release experiments are also an option but are too costly to be done in more than a handful of locations). Previous analyses of drifter trajectories from the Southern Ocean (e.g., Sallée et al. 2008; Griesel et al. 2010) did not detect such mixing suppression across mean flows.

As seen in KFLM and with the present stochastic model, the Lagrangian velocity autocorrelation is comprised of an exponentially decaying part and an oscillatory part; the latter depends on the phase speed of the eddies relative to the mean flow. If eddies and mean flow propagate at different speeds, the oscillatory part produces a negative lobe in the autocorrelation; this disappears when the eddies and mean flow propagate at the same speed. The negative lobe leads to a suppression of mixing, because it contributes negatively to the integral of the autocorrelation, which is the diffusivity.

The velocity autocorrelation is often found to have a negative lobe or equivalently the Lagrangian diffusivity reaches a maximum value before decreasing, so this aspect is not specific to the Southern Ocean. Because the error in the autocorrelation increases as the lag to one-half power (Davis 1991) and as floats drift into other regions with potentially different mixing, it is desirable to truncate the interval over which the autocorrelation function is computed, as noted previously. A standard practice is to integrate the autocorrelation to the first zero crossing (e.g., Freeland et al. 1975; Krauss and Böning 1987; Poulain and Niiler 1989; Lumpkin and Flament 2001; Lumpkin et al. 2002), equivalent to taking the maximum diffusivity. With mean flow suppression, this will produce an overestimate of the diffusivity. An alternate approach is to integrate to a fixed, intermediate time (e.g., Colin de Verdiere 1983; Brink et al. 1991; Speer et al. 1999; Griesel et al. 2010; Koszalka et al. 2011). If the upper limit of integration is large enough to encompass the negative lobe, this can be a satisfactory approach. However, to properly sample the negative lobes in the ACC, one must integrate to time lags on the order of 2 months in the ACC and longer to the north. Using a shorter limit will necessarily miss the suppression. An alternate method is to fit the autocorrelation with a function that is the product of an exponential and a cosine (Garraffo et al. 2001; Sallée et al. 2008). The fit determines the two time scales, for the decay and the oscillation [our $k(c_w - U)$ and γ]. Such an approach is perhaps most consistent with the present study but is also subject to errors in the autocorrelation at longer lags and does not alleviate the float number requirements.

In any case, it may well be difficult to obtain accurate estimates of eddy diffusivities from float statistics alone (for a more detailed discussion on necessary float statistics, see KFLM). Rather, one needs to combine float trajectories with additional information, such as the release of tracer patches, satellite-derived geostrophic velocities together with equivalent-barotropic scaling arguments, or high-resolution numerical models.

Last, our theory is based on homogeneous eddy statistics and hence relies on a scale separation between the flow and eddy (Corrsin 1974; Papanicolaou and Pironneau 1981). Its applicability to the ACC hinges on the broadness of the mean flow compared to the eddies. The remarkable agreement between the theory and diagnostic indicates that the former is indeed applicable locally to the ACC, in the sense of Wentzel–Kramers–Brillouin (WKB; Bender and Orszag 1978). However, the diagnostics are based on the altimetric velocity field, which is too coarse to fully resolve the sharp jets that straddle the ACC. Whether the theory remains applicable with a more strongly inhomogeneous environment, such

as the ACC with its sharp jets or the atmospheric jets whose width is comparable to or narrower than the scale of the embedded eddies, is an interesting question. Preliminary results based on high-resolution simulations and drifter observations suggest that the theory retains its skill, but departures are observed in the wake of major topographic features (Naveira Garabato et al. 2011; Sallée et al. 2011).

Acknowledgments. This work was done as part of the Diapycnal and Isopycnal Mixing Experiment in the Southern Ocean (DIMES). We wish to acknowledge the generous support of NSF through Award OCE-0825376 (RF and AK). We also wish to thank all the DIMES principal investigators for many useful discussions and suggestions and the two anonymous reviewers for their constructive comments.

APPENDIX

The Connection with Green (1970)

Green (1970) proposed a theory for PV fluxes in a horizontally homogeneous, baroclinically unstable flow based on the fastest growing linear normal mode. This idea was further developed as a full eddy parameterization scheme by Killworth (1997). The upshot of linear theory is that mixing by the most unstable mode in the quasigeostrophic approximation generates a diffusivity given by

$$K_{\text{linear}} = \frac{2k}{\kappa^2}\frac{c_i \text{EKE}}{c_i^2 + (U - c_r)^2}, \tag{A1}$$

where c_i and c_r are the imaginary and real speeds of the most unstable baroclinic mode. If one assumes that eddies decorrelate on a time scale proportional to their growth rate, $c_i \sim k^{-1}\gamma$, and propagate at the speed of the most unstable mode, $c_r = c_w$, then one recovers (19). Hence, Green's theory can be viewed as a special example of a general class of mixing models that account both for the finite eddy decorrelation time and for the eddy propagation speed.

REFERENCES

Abernathey, R., J. Marshall, M. Mazloff, and E. Shuckburgh, 2010: Critical layer enhancement of mesoscale eddy stirring in the Southern Ocean. *J. Phys. Oceanogr.,* **40,** 170–184.

Allen, D. R., and N. Nakamura, 2001: A seasonal climatology of effective diffusivity in the stratosphere. *J. Geophys. Res.,* **106,** 7917–7935.

Bender, C. M., and S. A. Orszag, 1978: *Advanced Mathematical Methods for Scientists and Engineers.* McGraw-Hill, 593 pp.

Bower, A. S., H. T. Rossby, and J. L. Lillibridge, 1985: The Gulf Stream—Barrier or blender? *J. Phys. Oceanogr.,* **15,** 24–32.

Brink, K., R. Beardsley, P. Niiler, M. Abbott, A. Huyer, S. Ramp, T. Stanton, and D. Stuart, 1991: Statistical properties of near surface currents in the California coastal transition zone. *J. Geophys. Res.,* **96,** 14 693–14 706.

Colin de Verdiere, A., 1983: Lagrangian eddy statistics from surface drifters in the eastern North Atlantic. *J. Mar. Res.,* **41,** 375–398.

Corrsin, S., 1974: Limitations of gradient transport models in random walks and in turbulence. *Advances in Geophysics,* Vol. 18A, Academic Press, 25–60.

Davis, R., 1991: Observing the general circulation with floats. *Deep-Sea Res.,* **38A,** S531–S571.

DelSole, T., 2004: Stochastic models of quasigeostrophic turbulence. *Surv. Geophys.,* **25,** 107–149.

Farrell, R., and P. J. Ioannou, 1993: Stochastic dynamics of baroclinic waves. *J. Atmos. Sci.,* **50,** 4044–4057.

Ferrari, R., and M. Nikurashin, 2010: Suppression of eddy diffusivity across jets in the Southern Ocean. *J. Phys. Oceanogr.,* **40,** 1501–1519.

Flierl, G. R., and D. J. McGillicuddy, 2002: Mesoscale and submesoscale physical-biological interactions. *The Sea: Ideas and Observations on Progress in the Study of the Seas,* A. R. Robinson, J. J. McCarthy, and B. Rothschild, Eds., *Biological-Physical Interactions in the Sea,* Vol. 12, John Wiley & Sons, 113–185.

Freeland, H., P. Rhines, and T. Rossby, 1975: Statistical observations of the trajectories of neutrally buoyant floats in the North Atlantic. *J. Mar. Res.,* **33,** 383–404.

Garraffo, Z., A. Mariano, A. Griffa, and C. Veneziani, 2001: Lagrangian data in a high-resolution numerical simulation of the North Atlantic. I. Comparison with in-situ drifter data. *J. Mar. Syst.,* **29,** 157–176.

Green, J. S. A., 1970: Transfer properties of the large-scale eddies and the general circulation of the atmosphere. *Quart. J. Roy. Meteor. Soc.,* **96,** 157–185.

Griesel, A., S. T. Gille, J. Sprintall, L. Mc, J. Clean, H. La, J. Casce, and M. E. Maltrud, 2010: Isopycnal diffusivities in the Antarctic Circumpolar Current inferred from Lagrangian floats in an eddying model. *J. Mar. Res.,* **66,** 441–463.

Haynes, P. H., and E. Shuckburgh, 2000a: Effective diffusivity as a diagnostic of atmospheric transport 1: Stratosphere. *J. Geophys. Res.,* **105,** 22 777–22 794.

——, and ——, 2000b: Effective diffusivity as a diagnostic of atmospheric transport 2: Troposphere and lower stratosphere. *J. Geophys. Res.,* **105,** 22 795–22 810.

Holloway, G., 1986: Estimation of oceanic eddy transports from satellite altimetry. *Nature,* **323,** 243–244.

——, and S. S. Kristmannsson, 1986: Stirring and transport of tracer fields by geostrophic turbulence. *J. Fluid Mech.,* **141,** 27–50.

Keffer, T., and G. Holloway, 1988: Estimating Southern Ocean eddy flux of heat and salt from satellite altimetry. *Nature,* **332,** 624–626.

Killworth, P. D., 1997: On the parameterization of eddy transfer. Part I: Theory. *J. Mar. Res.,* **55,** 1171–1197.

——, and C. W. Hughes, 2002: The Antarctic Circumpolar Current as a free equivalent-barotropic jet. *J. Mar. Res.,* **60,** 19–45.

Klocker, A., R. Ferrari, J. H. LaCasce, and S. T. Merrifield, 2012: Reconciling float-based and tracer-based estimates of eddy diffusivities. *J. Mar. Res.,* in press.

Koszalka, I., J. H. LaCasce, M. Andersson, K. A. Orvik, and C. Mauritzen, 2011: Surface circulation in the Nordic Seas from clustered drifters. *Deep-Sea Res. I,* **58,** 468–485.

Krauss, W., and C. W. Böning, 1987: Lagrangian properties of eddy fields in the northern North Atlantic as deduced from satellite-tracked buoys. *J. Mar. Res.,* **45,** 259–291.

Lumpkin, R., and P. Flament, 2001: Lagrangian statistics in the central North Pacific. *J. Mar. Syst.,* **29,** 141–155.

——, A.-M. Treguier, and K. Speer, 2002: Lagrangian eddy scales in the northern Atlantic Ocean. *J. Phys. Oceanogr.,* **32,** 2425–2440.

Marshall, J., E. Shuckburgh, H. Jones, and C. Hill, 2006: Estimates and implications of surface eddy diffusivity in the Southern Ocean derived from tracer transport. *J. Phys. Oceanogr.,* **36,** 1806–1821.

Mazloff, M. R., P. Heimbach, and C. Wunsch, 2010: An eddy-permitting Southern Ocean state estimate. *J. Phys. Oceanogr.,* **40,** 880–899.

Nakamura, N., 1996: Two-dimensional mixing, edge formation, and permeability diagnosed in area coordinates. *J. Atmos. Sci.,* **53,** 1524–1537.

——, and J. Ma, 1997: Modified Lagrangian-mean diagnostics of the stratospheric polar vortices 2. Nitrous oxide and seasonal barrier migration in the cryogenic limb array etalon spectrometer and SKYHI general circulation model. *J. Geophys. Res.,* **102,** 25 721–25 735.

Naveira Garabato, A. C., R. Ferrari, and K. L. Polzin, 2011: Eddy stirring in the Southern Ocean. *J. Geophys. Res.,* **116,** C09019, doi:10.1029/2010JC006818.

Ottino, J. M., 1989: *The Kinematics of Mixing: Stretching, Chaos, and Transport.* Cambridge University Press, 364 pp.

——, 1998: *Lectures on Geophysical Fluid Dynamics.* Oxford University Press, 378 pp.

Papanicolaou, G., and O. Pironneau, 1981: On the asymptotic behavior of motion in random flows. *Stochastic Nonlinear Systems,* L. Arnold and R. Lefever, Eds., Springer, 36–41.

Pedlosky, J., 1987: *Geophysical Fluid Dynamics.* 2nd ed. Springer-Verlag, 710 pp.

Poulain, P.-M., and P. P. Niiler, 1989: Statistical analysis of the surface circulation in the California current system using satellite-tracked drifters. *J. Phys. Oceanogr.,* **19,** 1588–1603.

Prandtl, L., 1925: Bericht über Untersuchungen zur ausgebildeten Turbulenz. *Z. Angew. Math. Mech.,* **5,** 136–139.

Rose, H. A., 1977: Eddy diffusivity, eddy noise, and subgridscale modelling. *J. Fluid Mech.,* **81,** 719–734.

Sallée, J. B., K. Speer, R. Morrow, and R. Lumpkin, 2008: An estimate of Lagrangian eddy statistics and diffusion in the mixed layer of the Southern Ocean. *J. Mar. Res.,* **66,** 441–463.

——, ——, and S. R. Rintoul, 2011: Mean-flow and topographic control on surface eddy-mixing in the Southern Ocean. *J. Mar. Res.,* **69,** 753–777.

Shuckburgh, E., and P. Haynes, 2003: Diagnosing transport and mixing using a tracer-based coordinate system. *Phys. Fluids,* **15,** 471, doi:10.1063/1.1610.

Speer, K., J. Gould, and J. LaCasce, 1999: Year-long float trajectories in the Labrador Sea Water of the eastern North Atlantic Ocean. *Deep-Sea Res. II,* **46,** 165–179.

Taylor, G. I., 1921: Diffusion by continuous movements. *Proc. London Math. Soc.,* **20,** 196–211.

Toole, J. M., and T. J. McDougall, 2001: Mixing and stirring in the ocean interior. *Ocean Circulation and Climate: Observing and Modelling the Global Ocean,* G. Siedler, J. Church, and J. Gould, Eds., Academic Press, 337–356.

Tulloch, R., J. Marshall, and K. S. Smith, 2009: Interpretation of the propagation of surface altimetric observations in terms of planetary waves and geostrophic turbulence. *J. Geophys. Res.,* **114,** C02005, doi:10.1029/2008JC005055.

Veneziani, M., A. Griffa, A. M. Reynolds, and A. J. Mariano, 2004: Oceanic turbulence and stochastic models from subsurface Lagrangian data for the northwest Atlantic Ocean. *J. Phys. Oceanogr.,* **34,** 1884–1906.

Wunsch, C., 2010: Toward a midlatitude ocean frequency–wavenumber spectral density and trend determination. *J. Phys. Oceanogr.,* **40,** 2264–2281.